

**Portfolio**

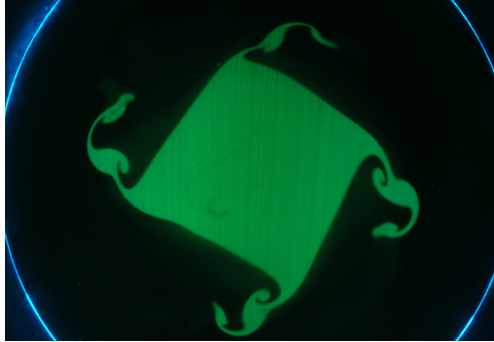
**Azimuthal Flow Patterns Produced by Annular Swirling Jets**

Adjovi, J.\* and Foucault, E.\*

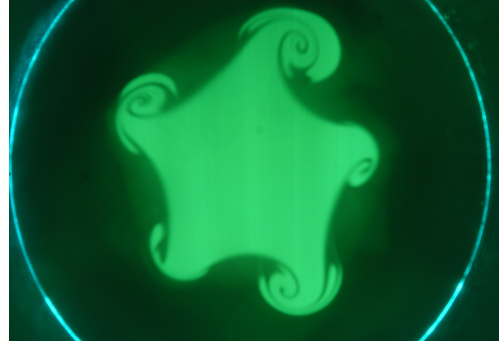
\* Laboratoires d'études Aérodynamiques, UMR CNRS Teleport 2, Bd Marie et Pierre Curie, BP30179 86962 Futuroscope Chasseneuil Cedex, France.

E-mail: joseph.adjovi@lea.univ-poitiers.fr / eric.foucault@lea.univ-poitiers.fr

Received 14 December 2006



$m = 4$ ,  $\xi = 2.5$ ,  $x/D_i = 4$ ,  $S = 0.6$  and  $Re = 2460$ .



$m = 5$ ,  $\xi = 3.75$ ,  $x/D_i = 4$ ,  $S = 0.2$  and  $Re = 3000$ .



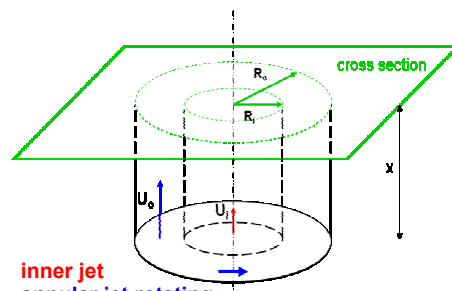
$m = 6$ ,  $\xi = 4.3$ ,  $x/D_i = 3$ ,  $S = 0.38$  and  $Re = 2460$ .



$m = 7$ ,  $\xi = 6.8$ ,  $x/D_i = 3$ ,  $S = 0.36$  and  $Re = 3600$ .



$m = 8$ ,  $\xi = 8.18$ ,  $x/D_i = 2$ ,  $S = 0.36$  and  $Re = 4000$ .



**inner jet**  
**annular jet rotating**  
 $R_i = 2$  cm : inner jet radius ( $D_i = 2 R_i$ )  
 $R_o = 5$  cm : annular jet radius  
 $U_o$  : axial velocity of annular jet  
 $U_i$  : axial velocity of inner jet  
 $x$  : axial position

Visualizations of azimuthal flow patterns of annular swirling jets by laser tomography at cross-sections of different axial positions  $x/D_i$  are shown here. There are two cylindrical coaxial jets where only the annular jet is rotating. This configuration commonly occurs in industrial burners. Slight

modifications of the flow parameters ( $\xi = \frac{\bar{U}_i}{U_o}$ ,  $S = \max\left(\frac{U_\theta(r)}{U_x(r)}\right)$  and  $Re = \frac{U_x D_i}{\nu}$  with  $U_x$  the axial mean velocity and  $D_i$  the inner jet diameter) give different vortex modes  $m \in \{4, 5, 6, 7, 8\}$ .

Portfolio

## Effect of a Neighboring Sonic Jet on the Shock Structure of a Sonic Jet

Vinoth, B. R.\* and Rathakrishnan, E.\*

\* Department of Aerospace Engineering, Indian Institute of Technology Kanpur, India.

Received 12 January 2007



(a) Top nozzle NPR 0, bottom nozzle NPR 3



(b) Top nozzle NPR 1.89, bottom nozzle NPR 3



(c) Top nozzle NPR 3, bottom nozzle NPR 3



(d) Top nozzle NPR 4, bottom nozzle NPR 3



(e) Top nozzle NPR 5, bottom nozzle NPR 3



(f) Top nozzle NPR 6, bottom nozzle NPR 3

The shadowgraph pictures show the changes in the shock-cell structure of a sonic jet of a fixed nozzle pressure ratio (NPR) due to a near by sonic jet at different NPR. Two identical axi-symmetric convergent nozzles of exit diameter ( $D$ ) 10 mm, placed with centre-to-centre distance of  $2.4D$ , were used in the experiments. The nozzles were connected to individual stagnation chambers so as to maintain different NPR for each nozzle. The NPR of the bottom nozzle was kept constant at 3. The top nozzle NPR was varied from 0 to 6.

The bottom jet shock-cells are influenced for top jet NPR 1.89, 3, and 4. For the top jet NPR 5 and 6 the bottom jet shock-cells are almost identical to the no flow condition in top nozzle. There is almost no change in the first 3 shock-cells for all the combinations tested. The maximum influence is observed for top jet NPR 3. The change in the shock-cells in the bottom jet is due to interaction of acoustic fields which depends on the expansion level of the jet, resulting in the modification of the acoustic feedback loop.

## Portfolio

### Visualizing Wifi Using the Wifi Camera

Somlai-Fischer, A.\*<sup>1</sup>, Sjöln, B.\*<sup>2</sup> and Haque, U.\*<sup>3</sup>

\*1 Aether Architecture, Budapest, Hungary. E-mail: adam@aether.hu

\*2 Automata AB, Stockholm, Sweden. Email: bengt@automata.se

\*3 Haque Design+Research. Email: info@haque.co.uk

Received 25 January 2007

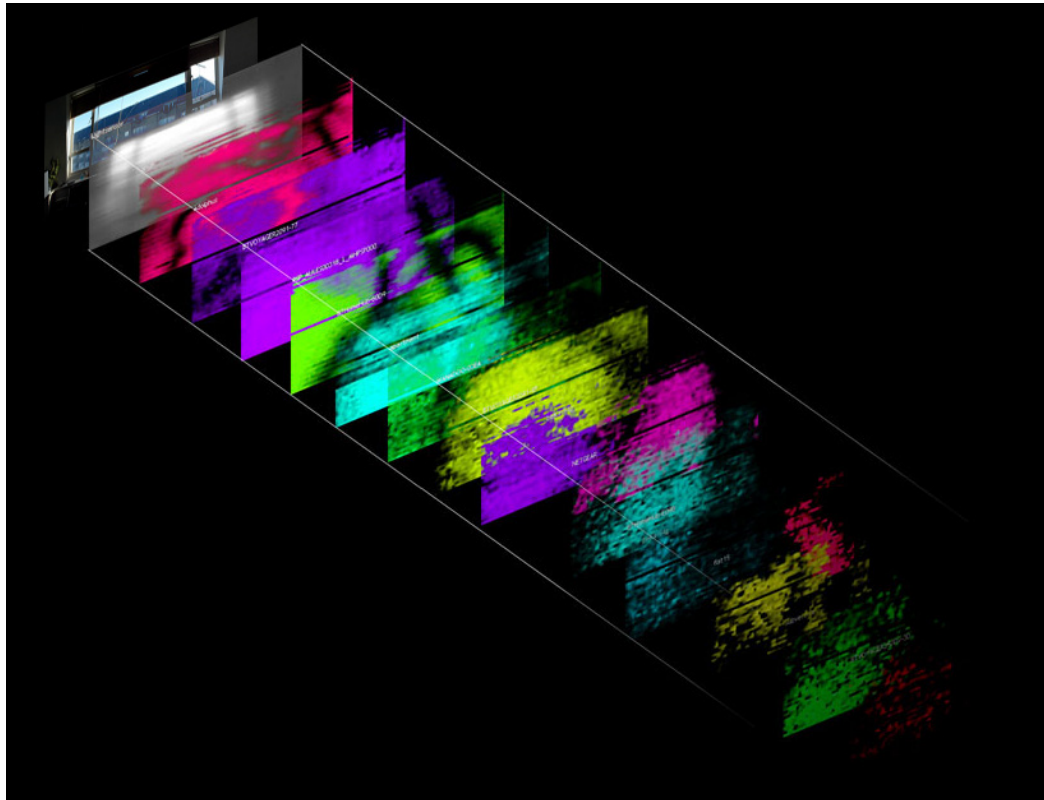


Fig. 1. Image of fifteen Wifi networks (each allocated an arbitrary colour) permeating a domestic living room.



Fig. 2. Equipment.



Fig. 3. View of two Wifi networks coming through a window (arbitrary colours).

These images were created using a “Wifi Camera” custom designed by Somlai-Fischer, Sjöln and Haque (information available at <<http://wificamera.propositions.org.uk/>>). It makes a use of a directional 2.4GHz wifi antenna mounted on servos scanning an environment at varying resolutions, measuring signal strength of all present networks to generate an image of the wifi “view” of the space. A light sensor is mounted on the antenna in order to generate a visible-light image that confirms precise orientation.

Portfolio

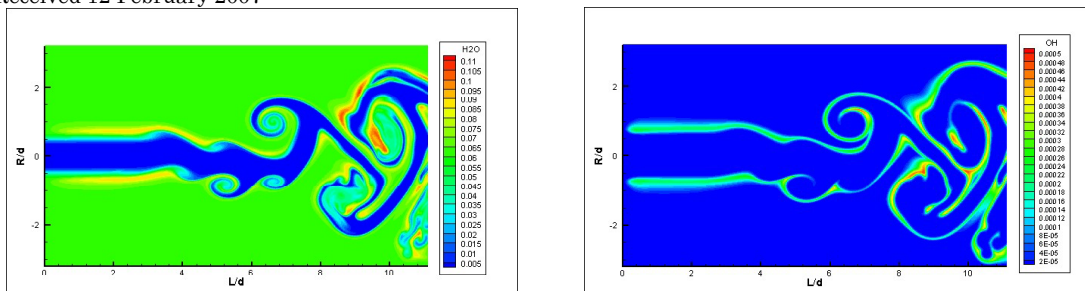
# Visualization of Nonpremixed Hydrogen Jet Flame in a Vitiated Coflow by DNS<sup>(1)</sup>

Wang, Z.\*, Zhou, J.\* and Cen, K.\*

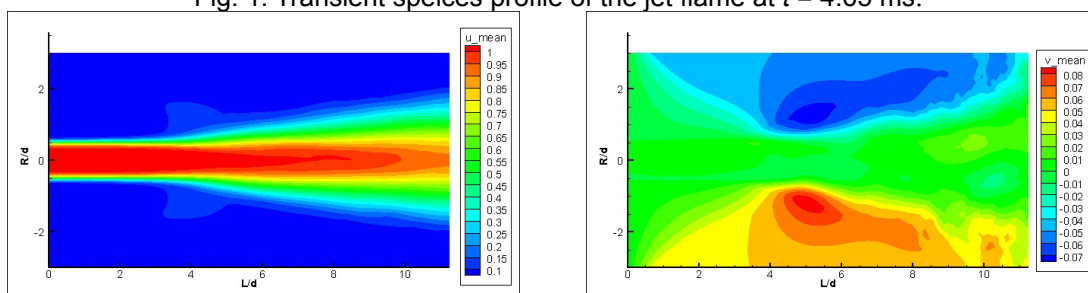
\* State Key Laboratory of Clean Energy Utilization, Institute for Thermal Power Engineering, Zhejiang University, Hangzhou, 310027, P. R. China.

E-mail: wangzh@zju.edu.cn

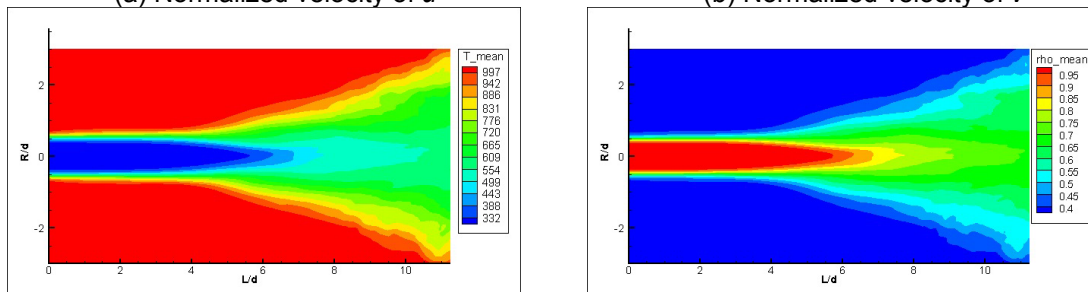
Received 12 February 2007



(a) Mass fraction of H<sub>2</sub>O (b) Mass fraction of OH  
Fig. 1. Transient species profile of the jet flame at  $t = 4.65$  ms.



(a) Normalized velocity of  $u$  (b) Normalized velocity of  $v$



(c) Temperature profile  $T$  (K) (d) Normalized density profile  $\rho$

Fig. 2. Favre averaged flow field of the jet flame. The reference values used here are: velocity  $u_r = 103.5$  m/s; density  $\rho_r = 0.856$  kg/m<sup>3</sup>

These figures show the simulation results of hydrogen jet flame in a vitiated coflow, which were realized by 2D DNS (Direct Numerical Simulation) method with 9 species and 16 steps chemical kinetic mechanism. The diameter of the jet is  $d = 4.57$  mm. The jet fuel is a mixture of 25 % H<sub>2</sub> and N<sub>2</sub> as dilution, by volume. The velocity of the jet is  $U_1 = 107$  m/s at 305 K. The coflow consisted of products from a lean premixed H<sub>2</sub>/air flame with a velocity of  $U_2 = 3.5$  m/s at 1045K. The composition is 15 % O<sub>2</sub>, 9.9 % H<sub>2</sub>O and 75 % N<sub>2</sub>, by volume. Based on the velocity of  $U_1 - U_2$ , jet diameter  $d$  and inlet fuel jet properties, the Reynold's number of the jet flame is 23000, Pr = 0.71. The autoignition phenomenon can be well captured and visualized. Figure 1 shows the transient mass fraction profiles of H<sub>2</sub>O and OH in the flow field, which were considered as the indicator of reaction as well as the heat release rate. The combustion mainly appears at the edge of the large scale vortex structures. At the end of the noncontinuous flame sheet or the positions with large curve rate, the combustion are always enhanced, as shown in Fig. 1(b). By accumulation of this kind of flame points, the fuel jet will be ignited automatically. Figure 2 shows the Favre-average results of velocity  $u$ ,  $v$ , temperature and density in the flow field.

<sup>(1)</sup> Supported by China Postdoctoral Science Foundation (20060391042) and National Science Foundation for Distinguished Young Scholars (50525620).